A simple method to evaluate the effectiveness of encapsulation materials for perovskite solar cells

Tim Wilderspin, Francesca De Rossi and Trystan Watson*[a]

SPECIFIC - Swansea University College of Engineering, Bay Campus, Swansea SA1 8EN, United Kingdom. E-mail: T.M.Watson@swansea.ac.uk

Abstract

Solution processed perovskite solar cells are an exciting development in the field of photovoltaics achieving power conversion efficiencies of over 20%. Nevertheless, stability issues are still limiting the successful entry of this technology into the PV market. Rapid degradation has been observed and reported as the result of different factors, such as light, humidity and temperature, simultaneously present during real operation. It is felt within the PV community that proper, effective encapsulation is one of the key contributors to increasing perovskite lifetimes. This work presents a simple and effective method based on RGB (red, green, blue) colour measurements to track perovskite degradation to lead iodide (PbI_2) using time lapse photography and thus evaluate the effectiveness/reliability of different encapsulation methods and materials. This technique gives a clear indication of when the perovskite has fully degraded and the impact of different encapsulants on degradation rate. This is supported by other analytical techniques, such as UV-Vis spectroscopy and XRD.

Keywords: perovskite, encapsulation, stability.

1. Introduction

Perovskite solar cells (PSC) present an exciting trend in the field of 3rd generation solar technologies [1, 2]. Within 4 years they have increased from 4% [3] power conversion efficiency (PCE) to over 20% [4]. They make use of solution processing resulting in potentially facile fabrication routes leading to manufacturing processes using scalable techniques such as bar coating and screen printing. However, major challenges to commercial uptake remain,

mainly related to the toxicity of the lead anion and the long term stability. The mesostructured PSC architecture, i.e. fluorine doped tin oxide/blocking layer/mesoporous oxide layer/($CH_3NH_3PI_3$ (MAPI) or $CH_3NH_3PbI_{3-x}Cl_x$ (MAPIC) perovskite/spiro-OMeTAD hole transport layer/gold, is understood to both quickly degrade in high humidity (>50% RH)[5] and be unstable in one sun light levels even in a moisture free environment [6]. Much work has been undertaken to improve the stability of PSCs [7, 5, 8, 9, 10, 11, 12, 13], either through changing layers within the PSC for more stable alternatives or trying to effectively encapsulate the cells from the external environment. Regarding the latter approach, Leijtens et al [14] were able to demonstrate almost completely stable photocurrent on glass and epoxy encapsulated alumina-based MAPIC cells, after light soaking for 1000 hours under 1 sun, AM1.5 illumination, at 40°C. The cells did however still suffer a 50% loss in efficiency in the first 200 hours, due primarily to losses in FF and Voc, likely related to the corrosion of the silver back contact. Hwang at al [15] reported a simple hydrophobic passivation process, using a Teflon layer applied via spin-coating, to increase PSC long term stability in air and ambient conditions for 30 days. The passivated cells even showed water-repellent property, when submerged under water for few seconds. Matteocci et al [16] employed a thermoplastic foil and a glass cover to encapsulate a MAPIC module. After an initial drop in the efficiency, the device showed to be stable for about 300 hours under 1 sun, AM1.5 irradiation, at 40°C. A more advanced encapsulation technique, borrowed from the organic light emitting diode (OLED) technology, consists of a cover glass and UV epoxy sealing with the addition of a piece of desiccant, placed below the cover glass, with the aim of absorbing any water that may permeate through the UV resin. This combination improved the device stability of MAPI cells [17, 18] but still significant degradation after prolonged aging at high temperature and humidity could be observed, mainly due to the decomposition of MAPI in the presence of water. In some cases, cell encapsulation and changes in working materials were combined, Habisreutinger et al [19] had success when they replaced the spiro-OMeTAD HTM with carbon nanotubes functionalised with P3HT and PMMA. Using these newly functionalised cells, they were able to demonstrate MAPIC cell stability even when exposed to running water and to temperature as high as 100°C. Mei et al [20] manufactured dual metal oxide PSCs, printing TiO_2, ZrO_2 and a 10 μm thick carbon back contact, which also served as an encapsulant, achieving over 1000 hours of stability in full sun conditions. It is clear that the width and breadth of encapsu-

lation materials that could apply to PSCs is large and will include at some point also very advanced techniques for thin film encapsulation, such as ALD and CVD, already developed and adopted for OLED and OPV [21, 22]. To test and prove their effectiveness on complete cells may require a long time and copious resources in terms of substrates and active materials. Here we present a direct and straight forward method for screening different encapsulants by using time lapse photography on perovskite layers only and the change in RGB values to monitor their degradation, the use of colour change as a tool for identifying degradation phenomena in solution processed solar cells has been used previously to demonstrate dye uptake and corrosion of metal substrates in dye-sensitized solar cells [23, 24, 25]. The RGB analysis is supported and confirmed by other analytical techniques, such as UV-Vis and XRD. Stability tests are finally carried out on complete cells, using only the most promising encapsulation solutions, thus saving time and materials.

2. Experimental

Figure 1 shows the layout of the different samples in the time lapse photography equipment, including four main groups of encapsulation materials: polymers in solution (PMMA and Polycarbonate), glass cover and epoxy resins (Torrseal top arrow, Alpha Adhesives SAS520 bottom arrow), glass covers and thermoplastic (Surlyn 25 μm), PET and pressure sensitive adhesive (PSA, Styccobond F46). Unless otherwise noted, the epoxy used throughout this work is the Alpha Adhesives SA5520 Marine Epoxy as both epoxies gave comparable results in initial studies. A cross section for each sample is also shown in order to highlight differences such as edge seal or overall layer.

All perovskite films were deposited onto FTO glass (Solaronix, TEC 7) via spin coating from a solution of $MAPbI_{3-x}Cl_x$ precursor (3:1 molar ratio of MAI to $PbCl_2$), 40%wt perovskite in DMF (99.8% anhydrous, Sigma Aldrich) and annealed for 90 minutes at 100°C and 10 minutes at 120°C. The edges of all samples were cleaned using a solution of chlorobenzene and DMF. Gaskets of 25 μm Surlyn (2.5 mm wide) were melted using a hot press at 100°C for 20 s to attach the glass cover on the samples. To obtain the same width of both epoxy seals, 0.3 ml of epoxy per sample were syringed around the edge of the perovskite. The PET films were double tape casted with PSA applied all over the area and dried on a hot plate for 70°C for 15 mins and 120°C for 5 mins. The polycarbonate (PC) and PMMA solutions were

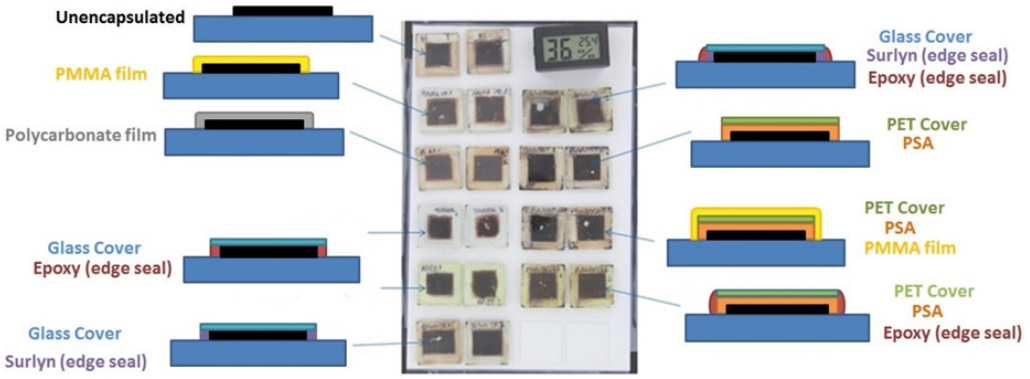

Figure 1: Sample location in the light box and cross sectional layout of each sample.

deposited via spin coating from a solution of 60 mg/ml PC in chlorobenzene and 50 mg/ml PMMA in toluene respectively. Both perovskite deposition and encapsulation were carried out inside a N_2 glovebox. The time lapse photography was completed in an Ortery Photosmile 200 light box, using a Canon EOS compact systems camera. The spectral output of the lightbox is 3580 lux, measured with a meter and is shown alongside the lightbox system itself in figure 2. We focused our work on these particular environmental conditions but irradiation, humidity and temperature can be changed, for example to meet ISOS standards [26] and the method will still be valid.

During the time lapse photography, images were captured every 10 minutes, the colour change analysis was performed using Sigmascan software which scanned a set area of each picture and returned the average RGB values. The completed cell stacks were manufactured on FTO glass by spraying a compact blocking layer from a 10% solution of TiAcAc (titanium diisopropoxide) in IPA sintered at 550°C for 60 minutes. A mesoporous titania layer was deposited via spin coating a commercial titania paste Dyesol 18NRT (diluted 2:7 parts by weight in ethanol) and sintered for 60 minutes at 550°C. The perovskite layer was deposited via spin coating from a solution of MAI (421mg/ml), $PbCl_2$(243mg/ml) and DMF and annealed for 90 minutes at 100°C and 10 minutes at 120°C in a N_2 atmosphere. The HTL was deposited via spin coating of a solution 8% by weight spiro-OMeTAD in chlorobenzene with 10 μl/ml tBP and 32 μl/ml of 600mM Li-TFSI in acetonitrile added. The Au contacts were evaporated using an Edwards 306 bell jar evaporator. J-V curves were measured on cells with an active area of 0.09 cm^2 under 1 sun using an Oriel Sol3A solar simulator (94023A). A Lambda

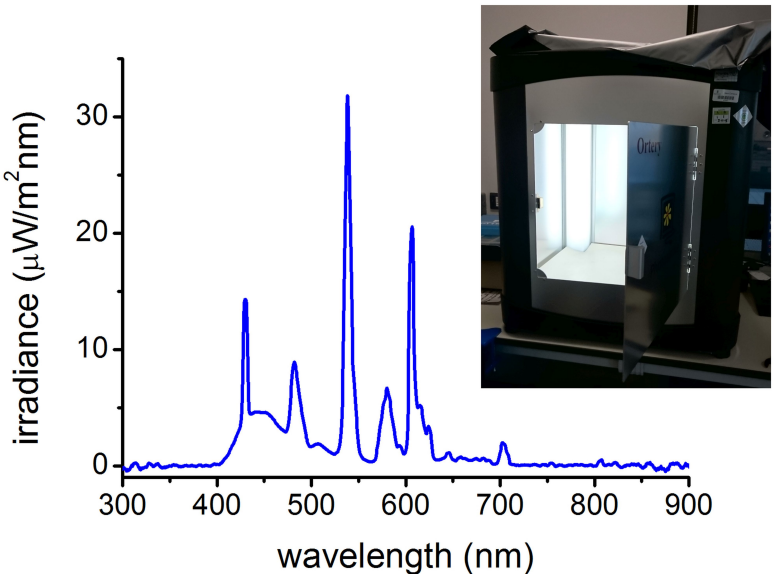

Figure 2: Light box spectral output. Inset: Time lapse setup

750S UV-vis-NIR spectrophotometer (Perkin Elmer) was used to measure the absorbance. X-ray diffraction data of perovskite films after different amounts of light soaking were collected on a D8 Discover (Bruker, Germany) X-ray diffractometer with a Cu $K\alpha$ source ($\lambda = 1.5418$ Å). The step time was 0.2s.

3. Results and Discussion

The degradation phenomenon being studied here is the decomposition of MAPIC films, catalysed by moisture and light, which leads to the formation of PbI_2 and to an evident change in film colour from black/dark brown to yellow [19], according to the reaction:

$$CH_3NH_3PbX_3 + H_2O \longleftrightarrow CH_3NH_3X(aq) + PbI_2(s)[27]$$

The RGB colour model is an additive system capable of expressing a vast array of colours with separate red, green and blue values. It has been adopted here to track precisely any changes in colour shown by the perovskite films and likely ascribable to the reaction shown above. Similarly to MAPIC, any other perovskite material, whose colour change is known to be associated with its degradation, such as methylammonium lead triodide [28] and mixed

iodide-bromide [29] can be analysed by RGB method The time lapse photography technique and RGB analysis of the automatically collected images presented here provide knowledge on the degradation timescales of perovskite layers when encapsulated and exposed to ambient conditions (room temperature, 30 to 40% humidity), under illumination from the compact fluorescent lights within the testing chamber at 3580 lux for over 1000 hours.

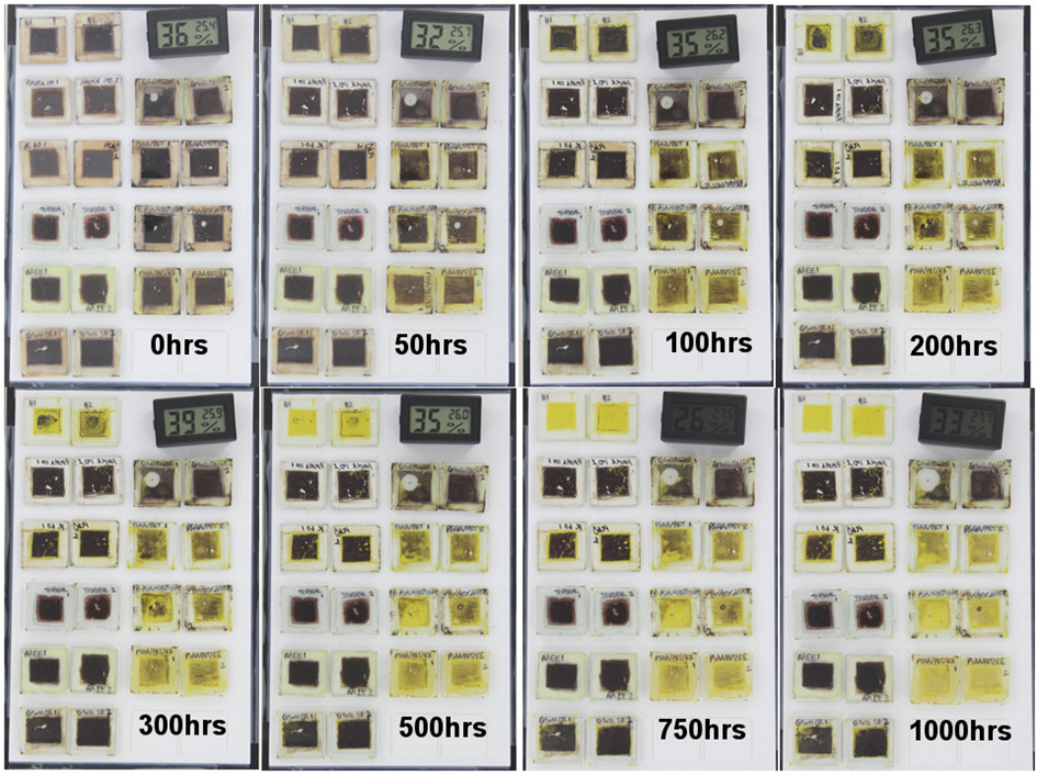

Figure 3: Photographic images produced at varying time intervals of perovskite films encapsulated using different methods. Unencapsulated samples are shown in the top left in each photo. Samples were maintained in a light box equipped with a camera and compact fluorescent lights, under ambient conditions.

Figure 1 shows the various combinations of encapsulants and the initial digital image. Subsequent images are shown in figure 3. From this we can see that non-encapsulated samples (first pair, top left) develop a slight change in colour, mainly around the edges, after 100 hours, whereas the PSA-based samples (three pairs from the bottom right) are already markedly degraded, likely due to the interaction between the solvent contained in the PSA itself,

casted all over the sample, and the perovskite. PC-covered samples (third pair from the top left) develop a small amount of yellowing (PbI_2 formation) from around 500 hours onwards, so do the Surlyn-based samples (last pair from the top left and first from the top right). In general the degradation progresses from the edges towards the centre, suggesting edge seal is critical, even when glass, a perfect barrier, is used as top encapsulation. PMMA and both epoxy resin encapsulation methods (second, fourth and fifth pair from top left) prove to protect effectively the perovskite film, preventing successfully PbI_2 formation. To quantify the degradation of the perovskite films and compare different encapsulation solutions, RGB changes for each couple of samples were extracted, using Sigmascan software which scanned a set area of each picture and returned the RGB values and plotted. To demonstrate this process figure 4 shows the RGB change of an unencapsulated MAPIC perovskite film over 1000 hours in the light box. Values from every 12 hours are presented for the first four days and every 24 hours for the rest of the test. After the initial drop observed for all colours in the first hundred hours, corresponding to an increase in the darkness of the perovskite colour, the average blue maintained an almost constant value while both average green and average red increased quickly until reaching a plateau from 500 hours onwards. Since the trend is similar for both and for the sake of clarity, the average green values only will be reported hereafter, as sufficiently representative of the overall change in colour of the perovskite film, generally from black/brown to yellow. The change in green colouration of all films over time is shown in figure 5.

The background RGB values were also taken into account to check for external factors which may have affected the data collection. Areas between two samples but including the glass on the sample edge were considered for the background RGB measurements since the bare glass substrates would not suffer any colour change unless deriving from external causes. Possible fluctuations of the bulbs irradiation over time inside the light box would be thus taken into account. No significant variation in the background readings with time and no presence of a significant dip (or darkening) in the first hundreds hours were observed. Still, the background values were subtracted from all the RGB plots reported hereafter. The dip in the average green value for the unencapsulated MAPIC film (Fig. 4 *b*) is also present in the epoxy- and PMMA-encapsulated samples, as reported afterwards. This seems to suggest that a real change takes place in the perovskite films, possibly a final curing step for the perovskite when exposed to light.

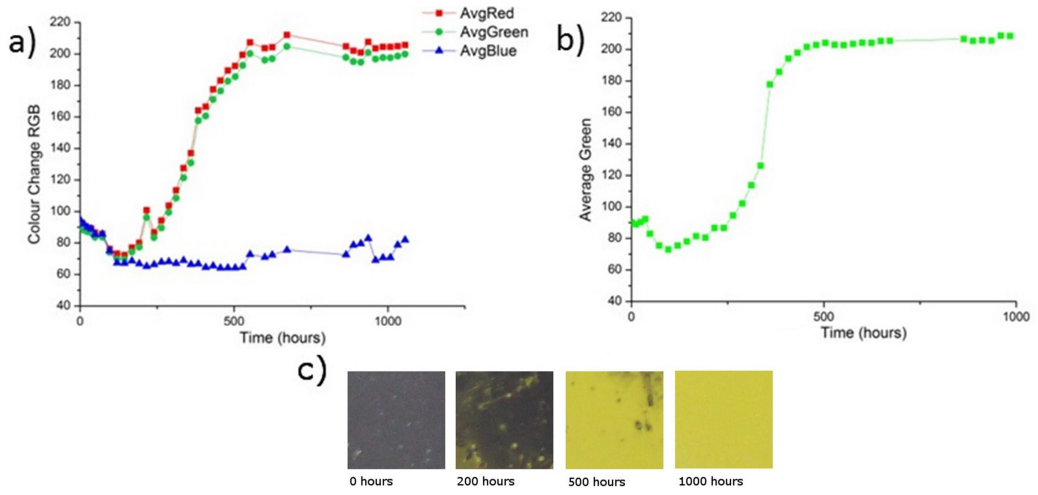

Figure 4: (a) RGB colour change of an unencapsulated perovskite sample over 1000 hours in the light box; (b) average green colour change of the same sample with the background variation removed, all other samples can be seen in figure 5 (c) Progressive colouration observed for unencapsulated samples

In order to confirm the degradation mechanism as that of the formation of PbI_2 XRD analysis was undertaken on two selected samples showing significantly different outcomes; the unencapsulated film, which had gone to yellow by 1000hrs and PMMA, which had maintained its original brown/black colour at 1000hrs, shown in figure 6. MAPIC perovskite peaks at 14 θ, 28 θ and 32 θ [17] progressively decrease for the unencapsulated samples whilst they remain stable for PMMA films, over the whole 1000 hour period. Interestingly, for both type of samples, the PbI_2 peak at 12.7 θ is present at the start of the experiment, confirming an incomplete conversion to MAPIC during the annealing of the films, prior to light soaking.

The evolution with time of the PbI_2 XRD peak, as a measure of the perovskite degradation rate, is reported in Figure 7 for the unencapsulated, PMMA- and polycarbonate-encapsulated samples. By 400 hours in the light box, the PbI_2 count in the unencapsulated sample reaches its maximum and is four and five times the amount in the polycarbonate and PMMA samples respectively. After 1000 hours, PMMA samples evolve less than 1.5 times their original amount of PbI_2, confirming the PMMA to successfully prevent moisture reaching the perovskite surface. The final PbI_2 count for the unencapsulated samples is approximately half that of the maximum count,

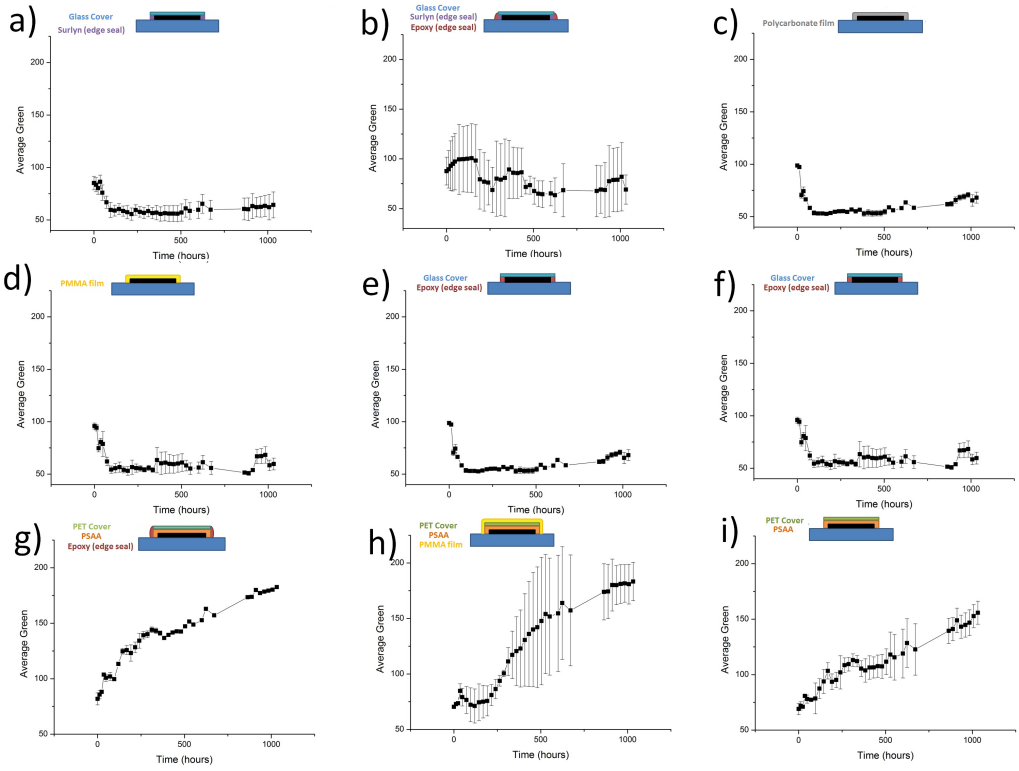

Figure 5: Change in average green colour of all samples show in figure 1. The key is a) Surlyn + Glass cover b) Surlyn + Glass cover + Alpha Adhesives Epoxy edge seal c) Polycarbonate d) PMMA e) Alpha Adhesives Epoxy + glass cover f) Torrseal epoxy + glass cover g)PSA + Alpha Adhesives epoxy edge seal h)PSA + PMMA i) PSA + PET

registered at 400 hours. This is on account of the perovskite being fully converted to PbI_2 and the PbI_2 then starting to break down and lose crystallinity to leave a smaller measurement at 12.7 θ .

Interestingly, a drop in the PbI_2 peak cannot be observed in the first hundred hours for any of the samples (Fig. 7), implying no final curing step has taken place inside the light box. More likely, lead iodide has been present in the unencapsulated samples from the beginning of light soaking and then additionally produced but it is not picked up by the colour change analysis until a significant amount of lead iodide causes a rapid change in colour. This confirms that the initial dip in Figure 4 for unencapsulated films and in figure 5 for other types of encapsulation is probably not linked to the amount of lead iodide in the samples. The PSA/PET samples only do not show any

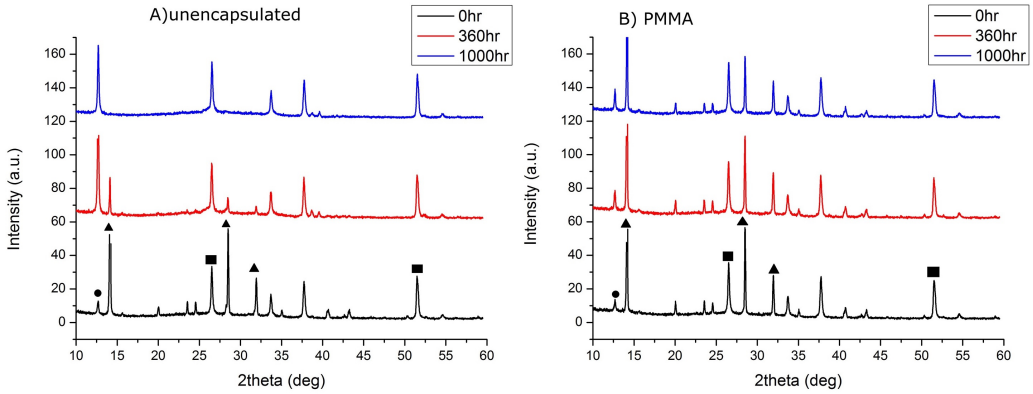

Figure 6: XRD Spectra for a) unencapsulated samples b) PMMA samples, showing the PbI_2 peak (solid circle), MAPIC perovskite peaks (solid triangles) and FTO peaks (solid squares).

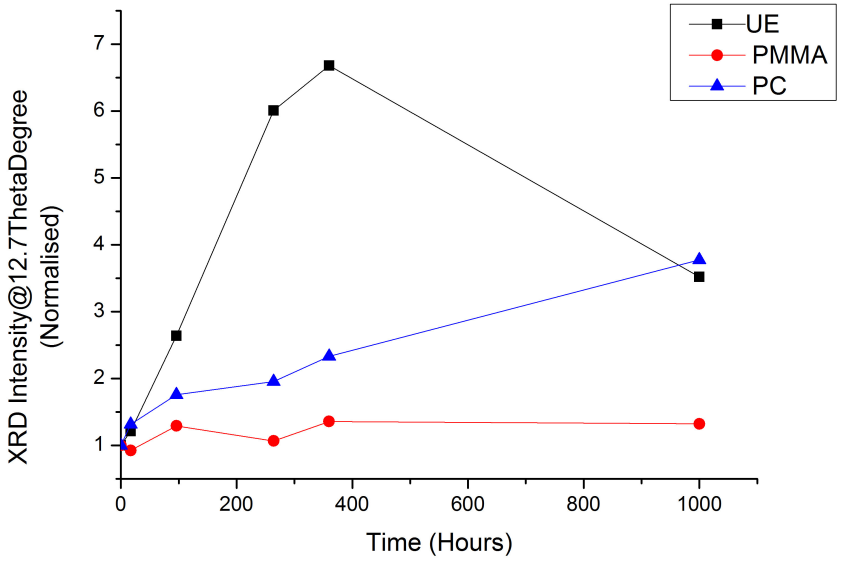

Figure 7: Change in lead iodide peak (12.7 θ) over time of the unencapsulated (UE), PMMA and polycarbonate (PC) samples.

dip, since PSA causes extremely rapid degradation, thus quick colour change, of the perovskite, probably due to additional oxygen and moisture trapped

within the PSA. By closely examining the time lapse photographs (figure 3), the degraded PSA-encapsulated samples appear only partially converted into PbI_2, revealing a possible inhomogeneity in the thickness of the bar casted adhesive: the degradation starts and is enhanced where the PSA is thicker. As a result, the colour change in the PSA samples is slower over all but quicker to begin with than the unencapsulated samples. To demonstrate the consistency of the RGB analysis, the optical absorbance of the same samples were recorded at different times. Figure 8 shows the change over time of both the average green value and the UV-Vis absorbance at 600 nm, the wavelength just below the first absorption peak for MAPIC perovskite, thus representing a crucial region, usually affected by a significant drop as confirmed by the UV-Vis spectra reported in figure S0. Small changes in average green and absorbance values lead to almost parallel lines, confirming a potentially successful encapsulation, namely PMMA and epoxy (Fig. 8, c and d). On the contrary, intersected curves mean MAPIC degradation to PbI_2 was observed, even if at different rates: the absorbance of PSA/PET samples (Fig. 8 b) decreased initially faster than the unencapsulated samples (Fig. 8 a) and after 350 hours at a slower rate.

In order to validate the effectiveness of the encapsulation methods discussed on the perovskite film component only, full cell stacks were encapsulated using glass covers and epoxy or Surlyn. Non-encapsulated cells were also prepared, as control/reference, and tested along with the encapsulated ones. PMMA solution was also employed, however the cells did not function following encapsulation, unfortunately the chlorobenzene used as solvent is incompatible with the spiro-OMeTAD layer. This expected result proves that a material passing the RGB analysis is only a potentially good encapsulant and highlights the need for further tests on complete cells after the preliminary screening on perovskite layers only. Stability tests in terms of power conversion efficiency were carried out on the devices, conducted by storing the cells both in the dark, at ambient conditions (room temperature, average RH of 60%), and under continuous illumination, at 3580 lux from fluorescent lamps, at room temperature and 34% average RH (figure S1). There is a dramatic difference between the dark and light soaking data. In the dark test, Surlyn-encapsulated and unencapsulated cells reported a similar drop in the efficiency (35-36%) after 1000 hours. The epoxy encapsulated cells instead lose less than 5% from their original PCE value, proving a better environmental barrier than Surlyn. When exposed to light soaking, all cells experienced faster and more severe degradation mainly ascribable to a drop

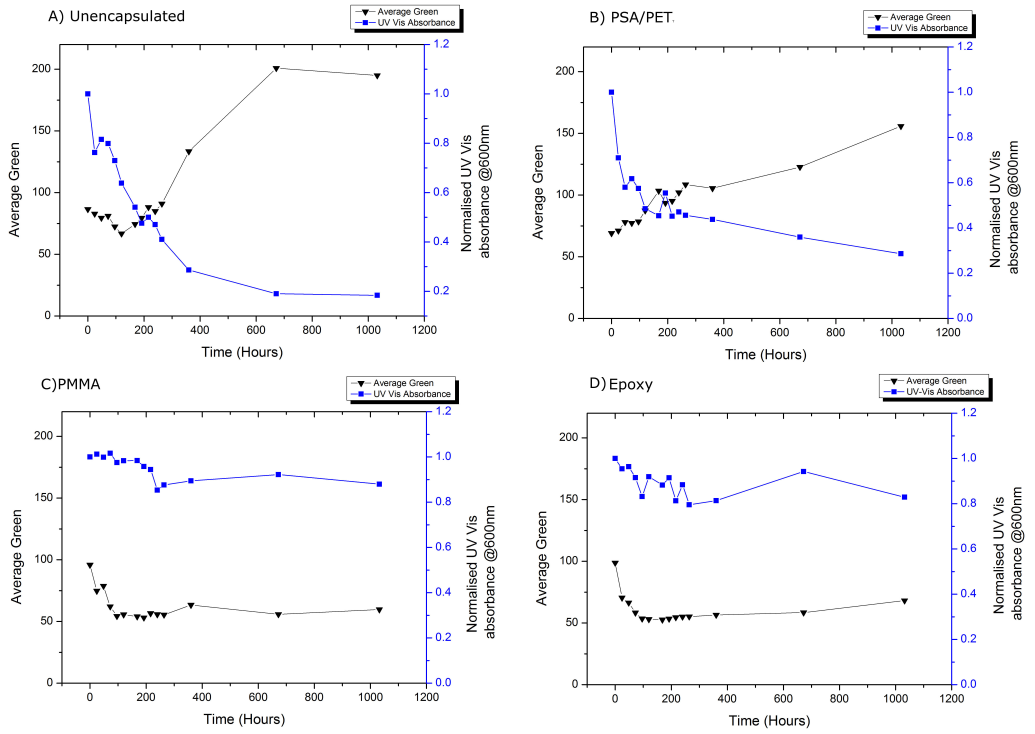

Figure 8: The average green colour change and normalised UV-Vis absorbance at 600 nm for a) unencapsulated, b) PSA/PET, c) PMMA and d) epoxy encapsulated perovskite films.

in photocurrent, which in turn can be linked to degradation of the perovskite and/or spiro-OMeTAD layer. Unencapsulated and Surlyn-encapsulated cells dropped to around one seventh of their original PCE within one day. The epoxy-encapsulated cells provided slightly more resistance with cells still giving small amounts of current after 350hours but still having dropped to less than half of their PCE in 120 hours. As the degradation took place in the encapsulated and unencapsulated alike, it is believed that a different component of the cell than the perovskite caused the degradation. RGB analysis of the whole device stack (figure S2) seems to validate this. The epoxy encapsulated cells showed very little sign of visual degradation, as reported by time lapse photography, still their performance degraded significantly (Figure S1.F), likely due to other faster or more severe degradation phenomena than the perovskite transformation into lead iodide. Further verification of this is however out of the scope of this work which aims to present a new

test method. Nevertheless, further in depth studies are ongoing.

4. Conclusions

This work presents a simple and effective method for studying the degradation of perovskite films via RGB colour analysis. By simply analysing the images taken at given intervals and extracting the RGB values, it provides a simple test for rapidly screening many types of encapsulation and discovering their potential effectiveness. The RGB analysis was supported by XRD and UV-Vis measurements which demonstrated the effectiveness of the method, in terms of simplicity and time-saving. If an encapsulant does not protect the perovskite layer, it is likely that it will not provide protection for complete cells either. Therefore, only few encapsulation solutions that passed the test were chosen as the most promising to be further tested in complete cells, reducing to less than one third the devices required for the experiment. Nevertheless, passing this test is a necessary but not sufficient condition for defining good encapsulation, as reported here for PMMA, epoxy resins and thermoplastic (Surlyn) when applied to complete cells. The devices demonstrated good RGB stability for single perovskite layers and even for complete devices if stored in air and dark at ambient conditions however they suffered a relevant drop in performance when exposed to light, in agreement with the literature for the same architecture of cells and set of materials.

5. Acknowledgements

The authors recognise the financial support of the EPSRC and Innovate UK for the SPECIFIC Innovation and Knowledge Centre (EP/N020863/1) the SuperSolar flexible funding (EP/J017361/1) and the Welsh Government for support for the Sêr Solar program.

6. References

[1] H.-S. Kim, C.-R. Lee, J.-H. Im, K.-B. Lee, T. Moehl, A. Marchioro, S.-J. Moon, R. Humphry-Baker, J.-H. Yum, J. E. Moser, M. Gratzel, N.-G. Park, Lead iodide perovskite sensitized all-solid-state submicron thin film mesoscopic solar cell with efficiency exceeding 9%, Scientific Reportsdoi:10.1038/srep00591.

[2] M. M. Lee, J. Teuscher, T. Miyasaka, T. N. Murakami, H. J. Snaith, Efficient hybrid solar cells based on meso-superstructured organometal halide perovskites., Science (New York, N.Y.) 338 (6107) (2012) 643–7. doi:10.1126/science.1228604.

[3] A. Kojima, K. Teshima, Y. Shirai, T. Miyasaka, Organometal halide perovskites as visible-light sensitizers for photovoltaic cells., Journal of the American Chemical Society 131 (17) (2009) 6050–1. doi:10.1021/ja809598r.

[4] M. A. Green, K. Emery, Y. Hishikawa, W. Warta, E. D. Dunlop, Solar cell efficiency tables (Version 45), Progress in Photovoltaics: Research and Applications 23 (1) (2015) 1–9. doi:10.1002/pip.2573.

[5] J. H. Noh, S. H. Im, J. H. Heo, T. N. Mandal, S. I. Seok, Chemical Management for Colorful, Efficient, and Stable InorganicOrganic Hybrid Nanostructured Solar Cells, Nano Letters 13 (4) (2013) 1764–1769. doi:10.1021/nl400349b.

[6] N. Aristidou, I. Sanchez-Molina, T. Chotchuangchutchaval, M. Brown, L. Martinez, T. Rath, S. A. Haque, The Role of Oxygen in the Degradation of Methylammonium Lead Trihalide Perovskite Photoactive Layers, Angewandte Chemie International Edition 54 (28) (2015) 8208–8212. doi:10.1002/anie.201503153.

[7] T. A. Berhe, W.-N. Su, C.-H. Chen, C.-J. Pan, J.-H. Cheng, H.-M. Chen, M.-C. Tsai, L.-Y. Chen, A. A. Dubale, B.-J. Hwang, Organometal halide perovskite solar cells: degradation and stability, Energy Environ. Sci. 9 (2) (2016) 323–356. doi:10.1039/C5EE02733K.

[8] B. Suarez, V. Gonzalez-Pedro, T. S. Ripolles, R. S. Sanchez, L. Otero, I. Mora-Sero, Recombination Study of Combined Halides (Cl, Br, I) Perovskite Solar Cells, The Journal of Physical Chemistry Letters 5 (10) (2014) 1628–1635. doi:10.1021/jz5006797.

[9] J.-W. Lee, D.-H. Kim, H.-S. Kim, S.-W. Seo, S. M. Cho, N.-G. Park, Formamidinium and Cesium Hybridization for Photo- and Moisture-Stable Perovskite Solar Cell, Advanced Energy Materials 5 (20) (2015) n/a–n/a. doi:10.1002/aenm.201501310.

[10] S. Aharon, A. Dymshits, A. Rotem, L. Etgar, Temperature dependence of hole conductor free formamidinium lead iodide perovskite based solar cells, J. Mater. Chem. A 3 (17) (2015) 9171–9178. doi:10.1039/C4TA05149A.

[11] A. Dubey, N. Adhikari, S. Venkatesan, S. Gu, D. Khatiwada, Q. Wang, L. Mohammad, M. Kumar, Q. Qiao, Solution processed pristine PDPP3T polymer as hole transport layer for efficient perovskite solar cells with slower degradation, Solar Energy Materials and Solar Cells 145 (2016) 193–199. doi:10.1016/j.solmat.2015.10.008.

[12] Y. S. Kwon, J. Lim, H.-J. Yun, Y.-H. Kim, T. Park, A diketopyrrolopyrrole-containing hole transporting conjugated polymer for use in efficient stable organicinorganic hybrid solar cells based on a perovskite, Energy & Environmental Science 7 (4) (2014) 1454. doi:10.1039/c3ee44174a.

[13] J. You, L. Meng, T.-B. Song, T.-F. Guo, Y. M. Yang, W.-H. Chang, Z. Hong, H. Chen, H. Zhou, Q. Chen, Y. Liu, N. De Marco, Y. Yang, Improved air stability of perovskite solar cells via solution-processed metal oxide transport layers, Nature Nanotechnology 11 (1) (2015) 75–81. doi:10.1038/nnano.2015.230.

[14] T. Leijtens, G. E. Eperon, S. Pathak, A. Abate, M. M. Lee, H. J. Snaith, Overcoming ultraviolet light instability of sensitized TiO with meso-superstructured organometal tri-halide perovskite solar cells., Nature communications 4 (2013) 2885. doi:10.1038/ncomms3885.

[15] I. Hwang, I. Jeong, J. Lee, M. J. Ko, K. Yong, Enhancing Stability of Perovskite Solar Cells to Moisture by the Facile Hydrophobic Passivation, ACS Applied Materials & Interfaces 7 (31) (2015) 17330–17336. doi:10.1021/acsami.5b04490.

[16] F. Matteocci, S. Razza, F. Di Giacomo, S. Casaluci, G. Mincuzzi, T. M. Brown, A. D'Epifanio, S. Licoccia, A. Di Carlo, Solid-state solar modules based on mesoscopic organometal halide perovskite: a route towards the up-scaling process, Physical Chemistry Chemical Physics 16 (9) (2014) 3918. doi:10.1039/c3cp55313b.

[17] Y. Han, S. Meyer, Y. Dkhissi, K. Weber, J. M. Pringle, U. Bach, L. Spiccia, Y.-B. Cheng, Degradation observations of encapsulated planar CH 3 NH 3 PbI 3 perovskite solar cells at high temperatures and humidity, J. Mater. Chem. A 3 (15) (2015) 8139–8147. doi:10.1039/C5TA00358J.

[18] F. Liu, Q. Dong, M. K. Wong, A. B. Djurišić, A. Ng, Z. Ren, Q. Shen, C. Surya, W. K. Chan, J. Wang, A. M. C. Ng, C. Liao, H. Li, K. Shih, C. Wei, H. Su, J. Dai, Is Excess PbI 2 Beneficial for Perovskite Solar Cell Performance?, Advanced Energy Materials (2016) n/a–n/adoi:10.1002/aenm.201502206.

[19] S. N. Habisreutinger, T. Leijtens, G. E. Eperon, S. D. Stranks, R. J. Nicholas, H. J. Snaith, Carbon Nanotube/Polymer Composites as a Highly Stable Hole Collection Layer in Perovskite Solar Cells, Nano Letters 14 (10) (2014) 5561–5568. doi:10.1021/nl501982b.

[20] A. Mei, X. Li, L. Liu, Z. Ku, T. Liu, Y. Rong, M. Xu, M. Hu, J. Chen, Y. Yang, M. Gratzel, H. Han, A hole-conductor-free, fully printable mesoscopic perovskite solar cell with high stability, Science 345 (6194) (2014) 295–298. doi:10.1126/science.1254763.

[21] J. Ahmad, K. Bazaka, L. J. Anderson, R. D. White, M. V. Jacob, Materials and methods for encapsulation of OPV: A review, Renewable and Sustainable Energy Reviews 27 (2013) 104–117. doi:10.1016/j.rser.2013.06.027.

[22] D. Yu, Y.-Q. Yang, Z. Chen, Y. Tao, Y.-F. Liu, Recent progress on thin-film encapsulation technologies for organic electronic devices, Optics Communications 362 (2016) 43–49. doi:10.1016/j.optcom.2015.08.021.

[23] T. Watson, P. Holliman, D. Worsley, Rapid , continuous in situ monitoring of dye sensitisation in dye-sensitized solar cells, Journal of materials chemistry 21 (2011) 4321–4325. doi:10.1039/c0jm03607b.

[24] T. Watson, G. Reynolds, D. Wragg, G. Williams, D. Worsley, Corrosion Monitoring of Flexible Metallic Substrates for Dye-Sensitized

Solar Cells, International Journal of Photoenergy 2013 (2013) 1–8. doi:10.1155/2013/791438.

[25] G. J. Reynolds, T. M. Watson, G. Williams, D. Worsley, Corrosion Resistance of Metallic Substrates for the Fabrication Dye-Sensitized Solar Cells, in: ECS Transactions, no. 17, pp. 129–138. doi:10.1149/1.3553355.

[26] M. O. Reese, S. A. Gevorgyan, M. Jørgensen, E. Bundgaard, S. R. Kurtz, D. S. Ginley, D. C. Olson, M. T. Lloyd, P. Morvillo, E. A. Katz, A. Elschner, O. Haillant, T. R. Currier, V. Shrotriya, M. Hermenau, M. Riede, K. R. Kirov, G. Trimmel, T. Rath, O. Inganäs, F. Zhang, M. Andersson, K. Tvingstedt, M. Lira-Cantu, D. Laird, C. McGuiness, S. J. Gowrisanker, M. Pannone, M. Xiao, J. Hauch, R. Steim, D. M. DeLongchamp, R. Rösch, H. Hoppe, N. Espinosa, A. Urbina, G. Yaman-Uzunoglu, J.-B. Bonekamp, A. J. van Breemen, C. Girotto, E. Voroshazi, F. C. Krebs, Consensus stability testing protocols for organic photovoltaic materials and devices, Solar Energy Materials and Solar Cells 95 (5) (2011) 1253–1267. doi:10.1016/j.solmat.2011.01.036.

[27] A. M. A. Leguy, Y. Hu, M. Campoy-Quiles, M. I. Alonso, O. J. Weber, P. Azarhoosh, M. van Schilfgaarde, M. T. Weller, T. Bein, J. Nelson, P. Docampo, P. R. F. Barnes, Reversible Hydration of CH 3 NH 3 PbI 3 in Films, Single Crystals, and Solar Cells, Chemistry of Materials 27 (9) (2015) 3397–3407. doi:10.1021/acs.chemmater.5b00660.

[28] D. Bryant, N. Aristidou, S. Pont, I. Sanchez-Molina, T. Chotchunangatchaval, S. Wheeler, J. R. Durrant, S. A. Haque, Light and oxygen induced degradation limits the operational stability of methylammonium lead triiodide perovskite solar cells, Energy Environ. Sci. 9 (5) (2016) 1655–1660. doi:10.1039/C6EE00409A.

[29] R. Ruess, F. Benfer, F. Böcher, M. Stumpp, D. Schlettwein, Stabilization of Organic-Inorganic Perovskite Layers by Partial Substitution of Iodide by Bromide in Methylammonium Lead Iodide, ChemPhysChem (2016) 1505–1511doi:10.1002/cphc.201501168.